Intermediate band position modulated by Zn addition in Ti doped $CuGaS_2$

Y. Seminóvski, P. Palacios , P. Wahnón

Instituto de Energía Solar and Dpt. Tecnologías Especiales, ETSI Telecomunicación, Universidad Politécnica de Madrid, 28040, Madrid, Spain

Keywords:
Chalcopyrite
Intermediate band materials
Electronic structure

A B S T R A C T

Many works have been done recently with the aim of obtaining intermediate band semiconductors, due to the significant importance of improving solar cell efficiency. Intermediate band materials based on $CuGaS_2$ chalcopyrite semiconductor are one of the proposed materials and specifically Ti doped $CuGaS_2$ is a promising structure to form the intermediate band. Here we present an *ab-initio* study using the density functional theory in this type of intermediate band chalcogens. Several concentrations of Ti and Zn substituting Ga atoms have been studied and their electronic densities of states were obtained. Results demonstrate a chalcopyrite semiconductor band-gap shortening and intermediate band position modulation inside this band-gap by Zn addition.

1. Introduction

At present, due to the remarkable interest in photovoltaic application, many ideas to increase solar cell efficiency have been developed as third generation solar cells. Between them the intermediate band concept is accepted, where there is a partially occupied band located inside a semiconductor band-gap, which can be used as an efficient solar cell.

The concept of the intermediate band (IB) refers to the presence of several energy levels constituting a narrow band, inside the band-gap and separated from the top of the valence band and conduction band bottom. This band allows the existence of two energy gaps, which originate absorption of two photons in addition to the photon absorbed in the host semiconductor band-gap; increasing, in this way, the absorption and making the photovoltaic material more efficient than before. The limiting efficiency of intermediate band solar cell is as high as $\eta = 0.632$ [1], greater than the calculated maximum theoretical efficiency of $\eta = 0.406$ [2] for a conventional solar cell with a single band-gap.

Due to the scarcity of experimental results related with synthesis of intermediate band solar cell semiconductor materials, the theoretical prediction of novel semiconductor materials of this type, which could face the solution of intermediate band semiconductor obtainment, is of great importance.

Chalcopyrite materials are one of the proposed semiconductors studied as host systems of the intermediate band. These materials have been widely investigated for many years [3–5] to be used in photovoltaic solar cells. The most important characteristic is that they combine advantages of thin film technology with the efficiency and stability of conventional crystalline silicon cells; this attractive behavior makes great expectation around future widespread use of solar cell chalcopyrites [5].

In our group, we have proposed some transition metal doped semiconductors (TMS) [6–9] as intermediate band materials. These earlier works [8,9] have revealed that the insertion of Ti into a chalcopyrite semiconductor such as $CuGaS_2$, with a band-gap found experimentally as 2.53 eV [10] depicts a separated intermediate band.

On the other hand, Zn in $CuGaS_2$ photoluminescence spectra having the form of $(CuGaS_2)_{1-x}$-$(2ZnS)_x$ have been experimentally measured [11,12] where a photoluminescence transition of 2.1–2.3 eV is reported (when x is 0.05–0.0005, respectively). This transition is ascribed to the band-gap of the heavily Zn doped $CuGaS_2$ in the Ga position, showing that there is a dependence of band-gap constriction when Zn concentration increases. In those past experimental works an amphoteric behavior of Zn impurity is also shown.

In agreement with the scope previously reviewed, which involves chalcopyrite characteristics combined with intermediate band formation in transition metal doped semiconductors and Zn effect into $CuGaS_2$, we present in this work Zn addition effect on Ti doped $CuGaS_2$ intermediate band systems, and its influence in the modulation of intermediate band inside doped semiconductors. We have to remark, that there is a necessity to isolate the intermediate band from the conduction band lower level in systems like Ti doped $CuGaS_2$, to avoid non-radiative recombination.

2. Models and methods

First, *ab-initio* density functional theory (DFT) calculations have been carried out on a representative structure consisting on a supercell derived from the parent body-centered tetragonal $CuGaS_2$ structure. Different dilutions of the proposed dopants inside the host semiconductor were computed. Supercells of different sizes were

constructed to achieve the desired proportion inside the semiconductor material; particularly, calculations with 32, 48 and 64 atom cells were carried out and compared. The dilutions proposed here were achieved by substituting Ti in a Ga position inside a $CuGaS_2$ supercell; further substitution with Zn as dopant was also performed replacing Zn in the Ga position.

Relaxed calculations and subsequent total and projected densities of states (DOS and PDOS) for different dilutions of the two metal dopants were carried out using the DFT VASP code, including spin polarization, with PAW potentials and the PW91 GGA functional [13–16]. A cutoff of 280 eV was applied for the plane-wave expansion and the Brillouin zone was sampled using $8\times8\times8$, $6\times6\times6$ and $8\times8\times6$ Monkhorst–Pack grids for the 32, 48 and 64 atom supercells, respectively. In all DOS figures, the Fermi energy level in the x-axis is set up at zero, and in y-axes, majority and minority spin states are positive and negative values respectively. In 32 and 48 atom supercells were found correspondingly 256 and 144 irreducible k points; 96 k points for the Ti in Ga symmetrical positions and 192 irreducible k points using Ti in Ga non-symmetrical positions were observed for the 64 atom supercells. In order to compare subsequent results, the same k point grid was taken for the two 64 atom supercells, and a comparative visualization of the two structures found after calculation appears in Fig. 1.

We name here, $Ti_2Cu_{16}Ga_{14}S_{32}$ and $ZnTi_2Cu_{16}Ga_{13}S_{32}$ to the 64 atom supercells having Ti in Ga symmetrical positions; and $Ti_2Cu_{16}Ga_{14}S_{32}^*$ and $ZnTi_2Cu_{16}Ga_{13}S_{32}^*$; for the Ti in Ga non-symmetrical positions. The band-gaps of the reached structures are compared using DFT, but taking into account that the DFT method underestimates band-gap values.

Tables 1 and 2 show the Ti doped $CuGaS_2$ atomic distances and the Zn in Ti doped $CuGaS_2$ atomic distances, respectively. The comparison shows that Ti–Ti distances have almost the same value in 32 and 48 atom supercells and the Ti–Ti distance value in $Ti_2Cu_{16}Ga_{14}S_{32}$ is greater than the distances in $Ti_2Cu_{16}Ga_{14}S_{32}^*$.

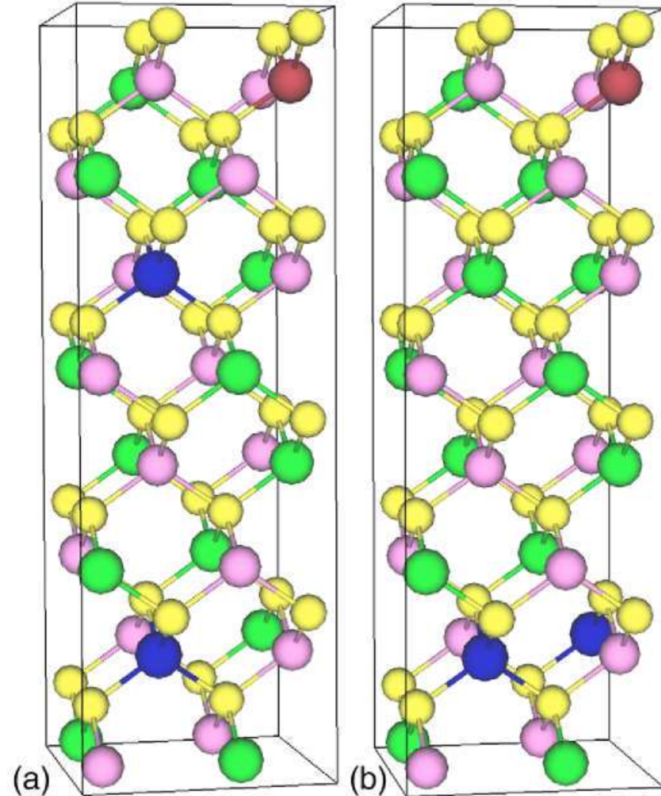

Fig. 1. 64 atom supercells with Ti (blue) substituted in different Ga (green) positions. In figures the atoms are: Zn (red), Cu (violet), and S (yellow). a) $ZnTi_2Cu_{16}Ga_{13}S_{32}$ and b) $ZnTi_2Cu_{16}Ga_{13}S_{32}^*$.

Table 1
Bond lengths in Ti doped $CuGaS_2$ structures for different dilutions found after relaxation (in Å).

	Ti–Ti	Ti–S	Ga–S_{min}	Ga–S_{max}	Cu–S_{min}	Cu–S_{max}
$Ti_2Cu_{16}Ga_{14}S_{32}$	7.58	2.35	2.32	2.33	2.30	2.32
$Ti_2Cu_{16}Ga_{14}S_{32}^*$	5.35	2.35	2.32	2.33	2.30	2.32
$Ti_2Cu_{12}Ga_{10}S_{24}$	6.56	2.35	2.31	2.34	2.29	2.32
$Ti_3Cu_{12}Ga_9S_{24}$	6.56	2.35	2.32	2.34	2.30	2.33
$Ti_2Cu_8Ga_6S_{16}$	6.57	2.35	2.32	2.34	2.30	2.32

Zn is added to the Ti doped $CuGaS_2$ in a way that forms the largest possible Zn–Ti distance, and Ti–Ti initial distances have been equally modeled in the systems with and without Zn doping. Besides, Zn–Ti distances are equal for the 32 and 48 atom supercells, and greater than those of 64 atom supercells. Also, Zn–Zn distances are almost equivalent for the 32 and 64 atom supercells, and different from the one with 48 atoms. Further discussion of the obtained distances after relaxing is presented in Table 2 and will be discussed in the next section.

3. Results and discussion

The $CuGaS_2$ starting structure, derived from the $A^IB^{III}C^{VI}$ chalcopyrite family structures confirms relation with the structure presented in natural zinc blende mineral, ZnS, and has the same D_{12}^{2D} tetragonal space group [17]. The bond distances Ga–S and Cu–S mean values in $CuGaS_2$ have been found, after relaxation, to be 2.33 and 2.31 Å respectively. These values are consistent with previously found experimental and theoretical values [17,18]. Table 1, shows comparison of Ga–S and Cu–S minimal and maximal distances found after relaxation in Ti doped compounds. No great differences are found when metal dilution changes. Also, the minimal and maximal values for each bond length have no significant difference between them.

Table 2 shows distances for the Zn and Ti doped $CuGaS_2$ structures. In this system, Ti–S, Cu–S and Ga–S bond length values have broader distribution than those found in Ti doped $CuGaS_2$, shown in Table 1. The minimal Cu–S and Ga–S bond length values were found for the nearest neighbors of Zn atoms. Each bond length distribution in studied cells was found similar, excluding 32 atom supercells where Zn and Ti atoms are substituting Ga position. It is important to point out that there are 8 total Ga atom positions, and three of them are substituted by two Ti and one Zn, which is a high doped proportion.

In this work, the DFT value for $CuGaS_2$ band-gap is 0.91 eV and for ZnS band-gap is 2.18 eV, demonstrating the consistency with chalcopyrite anomaly, due to the notable reduction on the $CuGaS_2$ band-gap compared with ZnS band-gap, having the same symmetry. Besides, the obtained band-gap value of Zn doped $CuGaS_2$ is 0.51 eV, which is a significant band-gap reduction for this system. This is consistent with a previous report of Zn in $CuGaS_2$ in the form of $(CuGaS_2)_{1-x}$-$(2ZnS)_x$ where the band-gap reduction is in a range of 0.23–0.43 eV related to the semiconductor band-gap. In this work, a

Table 2
Bond lengths in Zn and Ti doped $CuGaS_2$ structures for different dilutions found after relaxation (in Å).

	Ti–Zn	Zn–Zn	Ti–Ti	Zn–S	Ti–S_{min}	Ti–S_{max}	Ga–S_{min}	Ga–S_{max}	Cu–S_{min}	Cu–S_{max}
$ZnTi_2Cu_{16}Ga_{13}S_{32}$	6.53	7.58	7.58	2.34	2.32	2.35	2.27	2.36	2.28	2.33
$ZnTi_2Cu_{16}Ga_{13}S_{32}^*$	6.56	7.58	5.36	2.34	2.32	2.34	2.27	2.37	2.28	2.33
$ZnTi_2Cu_{12}Ga_9S_{24}$	5.32	10.70	6.53	2.34	2.33	2.35	2.28	2.35	2.28	2.33
$ZnTi_3Cu_{12}Ga_8S_{24}$	5.34	10.71	6.48	2.34	2.33	2.35	2.28	2.36	2.29	2.34
$ZnTi_2Cu_8Ga_5S_{16}$	5.34	7.55	6.58	2.31	2.35	2.36	2.30	2.33	2.31	2.33

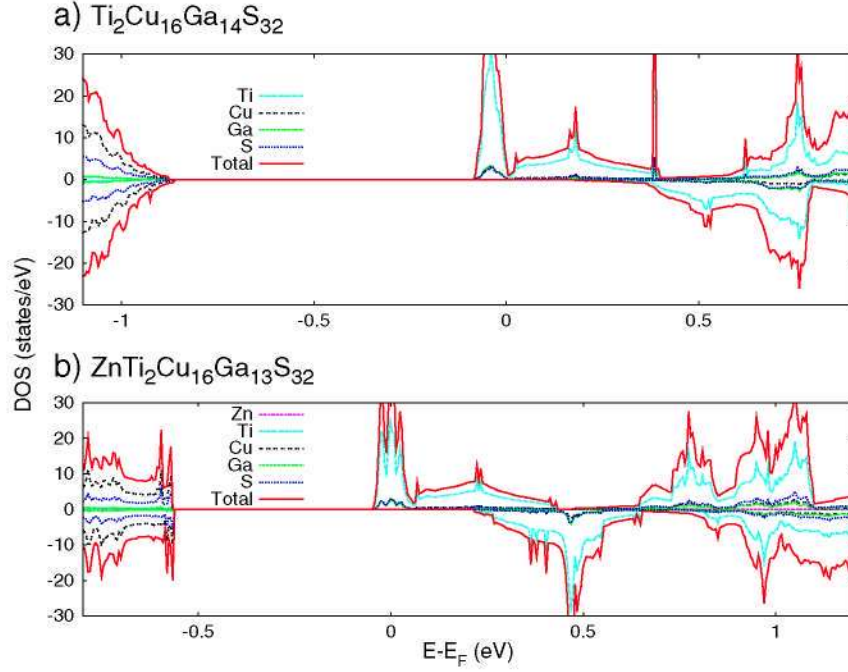

Fig. 2. DOS and PDOS for a) 6.25% Ti doped $CuGaS_2$ and b) 3.13% Zn in 6.25% Ti doped $CuGaS_2$ with Ti in Ga symmetrical positions.

band-gap shortening of 0.35 eV was obtained when 0.25% of Zn is added to the $CuGaS_2$ in a form of $ZnCu_8Ga_7S_{16}$.

Ti doped $CuGaS_2$ structures have been found highly spin polarized in all cases in agreement with previous works [8,9]. The intermediate band was also found, as is shown in section a) of Figs. 2 and 3 for a 6.25% concentration of Ti doped $CuGaS_2$ for the two different symmetries. These energy levels are potentially an intermediate band, even though a small density of states still appears between the upper intermediate band level and the lower level of the conduction band.

One unpaired spin per Ti in the primitive unit cell in all Ti doped structures was also found, demonstrating that Ti in the structure is in an oxidation state of Ti^{3+} and has an excess carrier of one electron per Ti substituted in the whole system. However, when Zn is added to Ti doped $CuGaS_2$, the unpaired spin disappears due to the expected Zn^{2+} oxidation state involved.

Tables 3 and 4 show the energy differences obtained in the DOS calculations, for the intermediate band of Ti doped $CuGaS_2$, and Zn in Ti doped $CuGaS_2$ for the equivalent structures, respectively. In these tables, $\varepsilon_C - \varepsilon_V$ is the value of the corresponding band-gap calculated

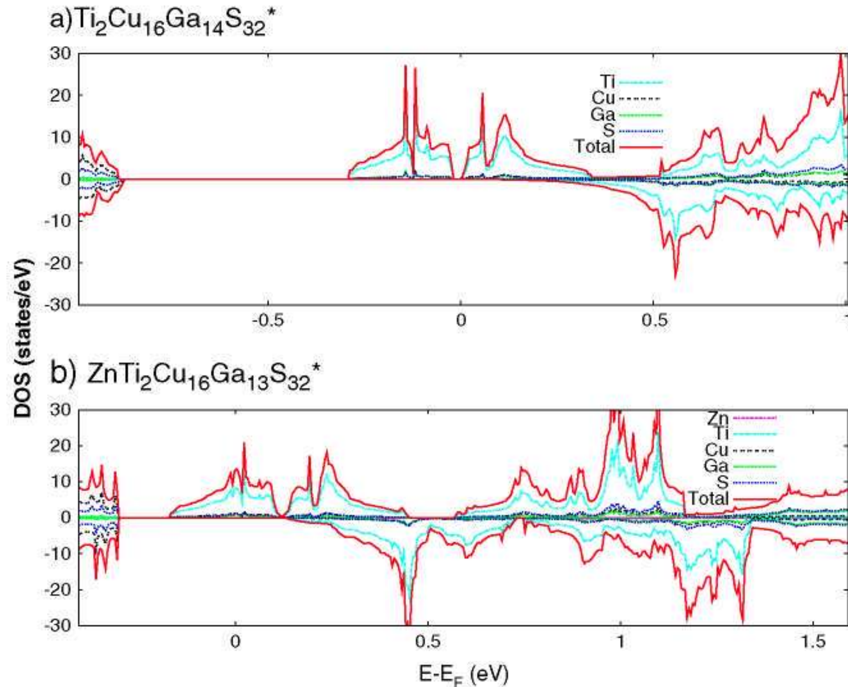

Fig. 3. DOS and PDOS for a) 6.25% Ti doped $CuGaS_2$ and b) 3.13% Zn in 6.25% Ti doped $CuGaS_2$ with Ti in Ga non-symmetrical positions.

Table 3
Energy level differences in Ti doped $CuGaS_2$ structures for different dilutions. Symbols are explained in the text (in eV).

	%Ti	$\varepsilon_C-\varepsilon_V$	$\varepsilon_{IBB}-\varepsilon_V$	IB_{width}
$Ti_2Cu_{16}Ga_{14}S_{32}$	6.25	1.05	0.800	Non isolated
$Ti_2Cu_{16}Ga_{14}S_{32}^*$	6.25	0.99	0.605	Non isolated
$Ti_2Cu_{12}Ga_{10}S_{24}$	8.30	1.10	0.770	Non isolated
$Ti_3Cu_{12}Ga_9S_{24}$	12.50	1.16	0.775	Non isolated
$Ti_2Cu_8Ga_6S_{16}$	12.50	1.18	0.775	Non isolated

Table 4
Energy level differences in Zn and Ti doped $CuGaS_2$ structures for different dilutions. Symbols are explained in the text (in eV).

	Ratio Zn/Ti	%Ti	%Zn	$\varepsilon_C-\varepsilon_V$	$\varepsilon_C-\varepsilon_{IBU}$	$\varepsilon_{IBB}-\varepsilon_V$	IB_{width}
$ZnTi_2Cu_{16}Ga_{13}S_{32}$	0.50	6.25	3.13	0.79	0.045	0.525	0.480
$ZnTi_2Cu_{16}Ga_{13}S_{32}^*$	0.50	6.25	3.13	0.49	0.125	0.140	0.620
$ZnTi_2Cu_{12}Ga_9S_{24}$	0.50	8.30	4.17	0.90	0.060	0.525	0.640
$ZnTi_3Cu_{12}Ga_8S_{24}$	0.30	12.50	4.17	0.94	0.120	0.570	0.660
$ZnTi_2Cu_8Ga_5S_{16}$	0.50	12.50	6.25	0.82	0.115	0.435	0.650

using the *spin down* levels, $\varepsilon_C-\varepsilon_{IBU}$ the energy difference between the conduction band lower level and the intermediate band upper level, and $\varepsilon_{IBB}-\varepsilon_V$ is the energy difference between the intermediate band lower level, and the valence band upper level. The last two energy differences were computed using the spin up levels; IB_{width} corresponds to the intermediate band width. We can infer from the comparison of the equivalent Zn in Ti doped $CuGaS_2$ and Ti doped $CuGaS_2$ structure results that when Zn is added in high proportion, further isolation of the intermediate band occurs. In Table 3, we can also compare the obtained band-gap value of different Ti doped $CuGaS_2$ structures with the computed $CuGaS_2$ band-gap of $\varepsilon_C-\varepsilon_V=0.91$ eV calculated in a similar way. This comparison leads to the conclusion that, when Ti is added to the semiconductor, all obtained band-gaps have a characteristic broadening. Then, when Zn is added to the already Ti doped $CuGaS_2$ chalcopyrite we can observe a band-gap reduction, showing the modulation effect of Zn, in Ti doped $CuGaS_2$ band-gap.

As we can deduce from Table 3, for the same Ti/Zn ratio in the compounds and excluding the $ZnTi_2Cu_{16}Ga_{13}S_{32}^*$ structure, when the Zn proportion increases, an increase of the $\varepsilon_C-\varepsilon_{IBU}$ width, a slight reduction in $\varepsilon_{IBB}-\varepsilon_V$ and a broadening of intermediate band are shown. If the Zn proportion rises from 3.3% to 4.17% we can see an increment in $\varepsilon_C-\varepsilon_V$; but, when the Zn proportion increases from 4.17% to 6.25% the band-gap is reduced by 0.12 eV.

The resulting DOS of Zn in Ti doped $CuGaS_2$ is depicted in Fig. 4, for 32 and 48 atom supercells. As it was demonstrated in the aforementioned tables, these systems show a displacement of the intermediate bands to energies away from the conduction band level and keeping the same

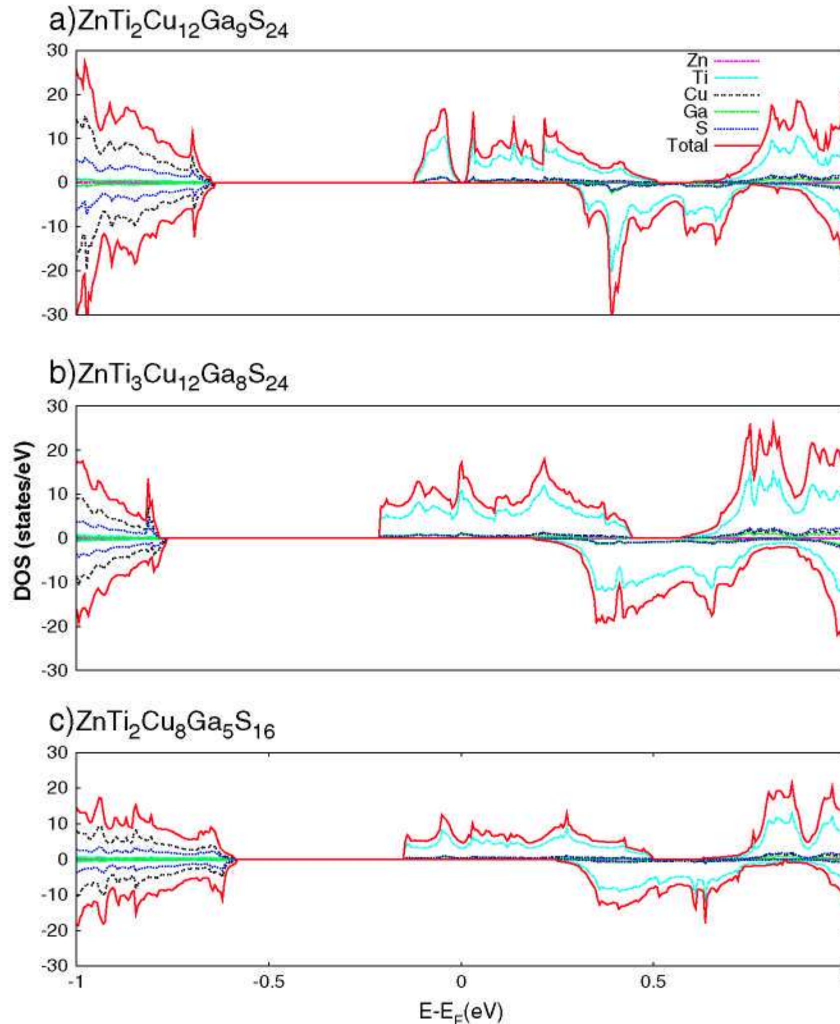

Fig. 4. DOS and PDOS for $ZnTi_2Cu_{12}Ga_9S_{24}$, $ZnTi_3Cu_{12}Ga_8S_{24}$, and $ZnTi_2Cu_8Ga_5S_{16}$ systems.

intermediate band width. This fact can be explained as the Zn energy levels in the formed materials are interacting directly in these intermediate bands. Although the intermediate band is mainly constituted of Ti atomic e_g orbitals, a slight proportion of Zn projected DOS appears contributing also in the intermediate band features of each dilution.

Variation of the substituent positions implies a variation of the band-gap and variation in the intermediate band features. This is shown for $ZnTi_2Cu_{16}Ga_{13}S_{32}$ and $ZnTi_2Cu_{16}Ga_{13}S_{32}$* in Figs. 2 and 3, where a comparison between both compounds in Figs. 2b) and 3b) shows a wider intermediate band and also a wider difference $\varepsilon_C - \varepsilon_{IBU}$ for $ZnTi_2Cu_{16}Ga_{13}S_{32}$*. Furthermore, $\varepsilon_{IBB} - \varepsilon_V$ energy difference in $Ti_2Cu_{16}Ga_{14}S_{32}$* and $ZnTi_2Cu_{16}Ga_{13}S_{32}$* has been found shorter than $\varepsilon_{IBB} - \varepsilon_V$ energy difference in the other calculated dilution. Moreover, greatly symmetric intermediate band peaks have been found, which can be related with the shorter Ti–Ti distance involved. Nevertheless, total energies of $Ti_2Cu_{16}Ga_{14}S_{32}$ and $ZnTi_2Cu_{16}Ga_{13}S_{32}$ have been found smaller than the corresponding total energies in $Ti_2Cu_{16}Ga_{14}S_{32}$* and $ZnTi_2Cu_{16}Ga_{13}S_{32}$*.

4. Conclusions

In this work, we present first principle calculations of Zn insertion effect in Ti:$CuGaS_2$ intermediate band materials. In agreement with previous experimental results [11,12], our results confirm than Zn reduces the host $CuGaS_2$ band-gap. Densities of states of different dilutions of Zn in Ti doped $CuGaS_2$ have been studied and discussed. The Zn substitution in Ti doped $CuGaS_2$ produces a distortion of the formed cell bond lengths, leading to changes in the densities of states inside the doped semiconductor.

In our results, we found that Zn modulates energies around the band-gap vicinity. In particular, the modulation effect consists in a separation of the intermediate band from the conduction band lower level, forming an isolated band structure. For a given Ti% and raising Zn concentration, results show approximately the same energy difference except for the $\varepsilon_C - \varepsilon_{IBU}$ value that shows a significant increase, caused mainly by Zn addition. This argument is also supported when we compare equal Ti doped $CuGaS_2$ structures with and without Zn doping. These statements show the Zn modulation effect in Ti doped $CuGaS_2$ and make the resulting Zn and Ti doped structures good materials to be proposed as intermediate band solar cells.

References

[1] A. Luque, A. Marti, Phys. Rev. Lett. 78 (1997) 5014.
[2] W. Shockley, H.J. Queisser, J. Appl. Phys. 32 (1961) 510.
[3] S. Wagner, J.L. Shay, P. Migliorato, H.M. Kasper, Appl. Phys. Lett. 25 (1974) 434.
[4] M. Wörz, E. Pschorr-Schoberer, R. Flierl, R. Preis, W. Gebhardt, J. Appl. Phys. 84 (1998) 2871.
[5] S. Siebentritt, U. Rau (Eds.), Wide Gap Chalcopyrites, Springer-Verlag, Berlin Heidelberg, 2006, p. 1.
[6] P. Wahnón, C. Tablero, Phys. Rev. B 65 (2002) 165115.
[7] P. Wahnón, P. Palacios, J.J. Fernández, C. Tablero, J. Mater. Sci. 40 (2005) 1383.
[8] P. Palacios, K. Sánchez, J.C. Conesa, P. Wahnón, Phys. Stat. Sol. 203 (2006) 1395.
[9] P. Palacios, et al., Thin Solid Films 515 (2007) 6280.
[10] B. Tell, J.L. Shay, J.H. Kasper, Phys. Rev. B 4 (1975) 2463.
[11] A. Ooe, Iida Seishi, Jpn. J. App. Phys. 29 (1990) 1484.
[12] A. Ooe, Tsuboi Nozomu, Iida Seishi, Jpn. J. App. Phys. 30 (1991) 2709.
[13] J.P. Perdew, Y. Wang, Phys. Rev. B 45 (1992) 13244.
[14] G. Kresse, J. Hafner, Phys. Rev. B 47 (1993) RC558.
[15] G. Kresse, J. Furthmüller, Phys. Rev. B 54 (1996) 11169.
[16] G. Kresse, J. Joubert, Phys. Rev. B 59 (1999) 1758.
[17] S. Laksari, A. Chahed, N. Abbouni, O. Benhelal, B. Abbar, Comp. Mat. Sci. 38 (2006) 223.
[18] J.E. Jaffe, A. Zunger, Phys. Rev. B 29 (1984) 1882.